PHYSICAL REVIEW D **89,** 043517 (2014)

Constraining anisotropic models of the early universe with WMAP9 data

S. R. Ramazanov[1,*] and G. I. Rubtsov[2,3,4,†]

[1]*Université Libre de Bruxelles, Service de Physique Théorique, CP225, Boulevard du Triomphe, B-1050 Brussels, Belgium*

[2]*Institute for Nuclear Research of the Russian Academy of Sciences, Prospect of the 60th Anniversary of October 7a, 117312 Moscow, Russia*

[3]*Physics Department, Moscow State University, Vorobjevy Gori 1, 119991 Moscow, Russia*

[4]*Novosibirsk State University, Pirogov street 2, 630090 Novosibirsk, Russia*

(Received 26 November 2013; published 19 February 2014)

We constrain several models of the early Universe that predict a statistical anisotropy of the cosmic microwave background (CMB) sky. We make use of WMAP9 maps deconvolved with beam asymmetries. As compared to previous releases of WMAP data, they do not exhibit the anomalously large quadrupole of statistical anisotropy. This allows us to strengthen the limits on the parameters of models established earlier in the literature. In particular, the amplitude of the special quadrupole is constrained as $|g_*| < 0.072$ at 95% C.L. ($-0.046 < g_* < 0.048$ at 68% C.L.) independently of the preferred direction in the sky. The upper limit is obtained on the total number of e-folds in anisotropic inflation with the Maxwellian term nonminimally coupled to the inflaton, namely $N_{\rm tot} < N_{\rm CMB} + 82$ at 95% C.L. ($+14$ at 68% C.L.) for $N_{\rm CMB} = 60$. We also constrain models of the (pseudo)conformal universe. The strongest constraint is obtained for spectator scenarios involving a long stage of subhorizon evolution after conformal rolling, which reads $h^2 < 0.006$ at 95% C.L., in terms of the relevant parameter. The analogous constraint is much weaker in dynamical models, e.g., Galilean genesis.

DOI: 10.1103/PhysRevD.89.043517 PACS numbers: 98.80.Cq, 98.80.Es

I. INTRODUCTION

The statistical isotropy of the cosmic microwave background (CMB) is one of the central pillars in modern cosmology. Manifesting the direction independence of the primordial spectrum at the onset of the hot era, it is renowned for its robustness against modifications in the bulk of inflationary models. Simple reasoning usually invokes the cosmic no-hair conjecture [1] which states the rapid isotropization of the Universe in the presence of a positive constant energy density. Scalar fluctuations (e.g., carried by the inflaton) evolve in the rotationally invariant metric and acquire a direction-independent spectrum, giving rise to the statistical isotropy of CMB temperature fluctuations. Clearly, a violation of this property observed in the CMB sky would indicate a nontrivial extension of currently conventional cosmology.

One way to break statistical isotropy is by introducing vector fields with nonvanishing vacuum expectation values [2–5]. For example, in the Ackermann-Carroll-Wise (ACW) model [2], the idea is to add a massive vector with a fixed space-like norm. This allows for the anisotropic evolution of the Universe which introduced the direction dependence into the power spectrum of the primordial curvature perturbation ζ. For future convenience, we write it in the generic form

$$\mathcal{P}_\zeta(\mathbf{k}) = \mathcal{P}_\zeta(k)\left(1 + a(k)\sum_{LM} q_{LM} Y_{LM}(\hat{\mathbf{k}})\right). \quad (1)$$

Here $\hat{\mathbf{k}}$ is the direction associated with the cosmological wave vector $\mathbf{k}$, the Y_{LM}'s are spherical harmonics, the q_{LM}'s are coefficients parametrizing the statistical anisotropy, and $a(k)$ is the direction-independent amplitude. In the ACW model, the amplitude $a(k)$ is constant, i.e., it can be tuned to unity without loss of generality. Furthermore, the predicted statistical anisotropy is of the quadrupole type, i.e., only the coefficients q_{2M} survive, which are not independent. In particular, by an appropriate choice of the reference frame, one can tune all the coefficients q_{2M} (except for q_{20}) to zero. The z axis of this reference frame is associated with the preferred direction in the sky. Hereafter, we use the term *special quadrupole* for this type of statistical anisotropy.

Soon afterwards, it was realized that the ACW model is unstable [6]. This is due to the longitudinal component of the massive vector that propagates as a ghost in the inflationary background. Similarly, all vector models of inflation violating gauge U(1) symmetry share the same problem [6]. This problem does not arise in the models of Ref. [7] that introduce the Maxwellian term modified by the explicit coupling to the inflaton. Remarkably, for quite a wide range of coupling functions and inflaton potentials, one can achieve the anisotropic expansion of the Universe [7] in a ghost-free manner [8]. (See also Refs. [9,10] for

*Sabir.Ramazanov@ulb.ac.be
†grisha@ms2.inr.ac.ru

reviews.) The outcome of anisotropic inflation is still the direction dependence of the ACW type, while the preferred direction is associated with the electric component of the electromagnetic field. Interestingly, the amplitude of the special quadrupole relies on the overall number of e-folds during inflation [11]. (See also Ref. [12].) In turn, this means that the duration of inflation in those models can be strongly constrained with the CMB data.

Statistical anisotropy may follow naturally from alternative frameworks, e.g., the (pseudo)conformal universe [13–15]. Minimal models of this type incorporate at least two fields: one—which we call ρ—with the conformal weight $\Delta \neq 0$, and the zero-weighted conformal field σ. In particular, the conformal rolling scenario [13] and Galilean genesis [14]—two known incarnations of the (pseudo) conformal universe—deal with the weight $\Delta = 1$ field ρ. We focus on this case in the present paper. The field ρ is then assumed to have the time-dependent solution

$$\rho_0 = \frac{1}{h(t_* - t)}, \tag{2}$$

spontaneously breaking the conformal group SO(4,2) down to the de Sitter subgroup SO(4,1). The constant h is the only relevant parameter of the conformal rolling scenario or Galilean genesis. The symmetry-breaking pattern $\mathrm{SO}(4,2) \to \mathrm{SO}(4,1)$ fixes the phenomenological properties of the weight-0 field perturbations $\delta\sigma$ evolving in the background (2) created by the field ρ. In particular—regardless of the precise details of the microscopic physics—one ends up with the scale-invariant power spectrum of the perturbations $\delta\sigma$ [15]. Thus, they may serve as the source of primordial fluctuations in the standard matter at the onset of the radiation-dominated (RD) stage.

The setup of the (pseudo)conformal universe leads unavoidably to a nonzero statistical anisotropy [16–18]. This originates from the interaction between weight-0 and weight-1 perturbations. There are two possible types of predictions depending on the state of cosmological perturbations at times when conformal symmetry becomes irrelevant. If they are already superhorizon at these times, the resulting direction dependence is of the quadrupole type akin to anisotropic inflation [16,18]. The structure of the statistical anisotropy is particularly rich in the situation with subhorizon cosmological perturbations [17]. In that case, all the coefficients q_{LM} with even L are generically nonzero in Eq. (1). In both cases, the direction dependence is governed by the constant h. This gives a simple idea of how to constrain the models of interest from the nonobservation of statistical anisotropy in the CMB sky.

Our main goal in the present paper is to constrain models of the early Universe that predict statistical anisotropy. We do this in the same manner as in our previous paper [19], where the conformal rolling scenario was constrained by making use of the WMAP7 data. Namely, we apply quadratic maximum likelihood (QML)-based estimators [20] to the CMB data and establish upper limits on model parameters. In the present paper, we turn to the WMAP9 maps. With the latter, there is a strong reason to anticipate much tighter constraints. We expect that the WMAP9 data lack the anomalously large quadrupolar statistical anisotropy observed in the W band of the 5-year release [21,22]. The anomaly was first interpreted as a hint towards the ACW model. However, the preferred direction of the signal was found to be highly aligned with poles of the ecliptic plane [20–22]. Its frequency dependence was also suspicious: the signal so prominent in the W band was much weaker in the V band [20]. Finally, results from alternative searches, i.e., large-scale structure surveys, favor statistically isotropic primordial perturbations [23]. These three points strongly indicate the systematic origin of the signal detected. In Ref. [20], it was suggested that beam asymmetries not accounted for in the previous analysis could strongly bias primordial statistical anisotropy. Indeed, upon the inclusion of beam asymmetries into the computational scheme, the large quadrupole statistical anisotropy vanishes. This was first shown in Ref. [24] for the W band of the WMAP7 data. To deal with this effect in the 9-year final data release, the WMAP Collaboration has produced the beam-symmetrized temperature maps [25].

This paper is organized as follows. In Sec. II we review vector models of inflation predicting statistical anisotropy. We focus on the particular class of scenarios with the Maxwellian term nonminimally coupled to the inflaton. We review models of the (pseudo)conformal universe in Sec. III. In Sec. IV we establish the estimators which are most appropriate for our constraining purposes. In Sec. V we apply the estimators to models of interest and obtain constraints on their parameters. We compare our constraints with similar bounds obtained from the Planck data in Sec. VI.

II. ANISOTROPIC INFLATION

In this section we briefly discuss inflationary scenarios which lead to statistical anisotropy. We focus on a particular class of slow-roll inflation that incorporates Abelian gauge fields with U(1) gauge symmetry. The healthy extension of inflation in terms of vectors is achieved by the following modification of the standard Maxwellian term [7]:

$$S_A = -\frac{1}{4}\int d^4x\sqrt{-g}\cdot f^2(\phi)\cdot F^{\mu\nu}F_{\mu\nu}.$$

Here $f(\phi)$ is some function of the inflaton φ, and $F_{\mu\nu}$ is the field strength of the vector field, $F_{\mu\nu} = \partial_\mu A_\nu - \partial_\nu A_\mu$. The main statement of Ref. [7] is that for quite a wide range of kinetic gauge functions $f(\phi)$ there is a chance of obtaining

a prolonged anisotropic evolution. That is, the space-time metric tends to the attractor solution

$$ds^2 = dt^2 - e^{2Ht}[e^{-4\Sigma t}dx^2 + e^{2\Sigma t}(dy^2 + dz^2)]. \quad (3)$$

Here Σ is the parameter which measures the deviation from the rotational invariance. Furthermore, the evolution of inflaton fluctuations in this "hairy" background (3) leads to a directional dependence of the ACW type in the primordial power spectrum. Here we write it in the conventional form,

$$\mathcal{P}(\mathbf{k}) = \mathcal{P}(k)(1 + g_*\cos^2\theta), \quad (4)$$

with θ being the angle between the wave vector $\mathbf{k}$ and the direction $\hat{\mathbf{E}}_{\rm cl}$ of the electric field $\mathbf{E}_{\rm cl}$ generated during the inflationary stage. The amplitude g_* is sourced by the electric field, i.e., $g_* \sim E_{\rm cl}^2$, as we discuss in more detail in what follows. The relationship between the power spectrum (4) and the generic one (1) is given by the relations

$$q_{2M} = \frac{8\pi g_*}{15} Y^*_{2M}(\hat{\mathbf{E}}), \qquad g_*^2 = \frac{45}{16\pi}\sum_M |q_{2M}|^2, \quad (5)$$

which are valid in the approximation of a small amplitude $g_* \ll 1$.[1] Note that $a(k) = 1$ in Eq. (1). To avoid confusion in the future, let us make one remark here. Though we use the terms "electric" and "magnetic," our definitions of the corresponding fields are different from the conventional ones. Namely [11],

$$E_i = -\frac{\langle f\rangle}{a^2}A_i', \qquad B_i = \frac{\langle f\rangle}{a^2}\epsilon_{ijk}\partial_j A_k,$$

where $\langle f\rangle$ denotes the expectation value of the function $f(\phi)$, and a prime denotes the derivative with respect to conformal time. With these definitions, the electromagnetic energy density is given by the standard expression $\rho_A = \frac{\mathbf{E}^2+\mathbf{B}^2}{2}$ at all times.

Let us discuss briefly the conditions at which statistical anisotropy is generated. In the situation with the standard Maxwellian term, i.e., provided that $\langle f\rangle = 1$, electric and magnetic fields fall down rapidly with time, as does the electromagnetic energy density ρ_A, which redshifts away as $\rho_A \propto a^{-4}$. This standard prediction can be avoided given the nontrivial structure of the function $f(\phi)$. A constant electric field is generated for the class of functions $f(\phi)$ defined by [7]

$$f(\phi) = e^{\frac{16c\pi}{M_{\rm Pl}^2}\int\frac{V}{V_\phi}d\phi}, \quad c > 1,$$

where $V(\phi)$ is the inflaton potential. In Ref. [7], the case $c = 1$ was argued to be the critical one, i.e., for $c < 1$ the Universe is statistically isotropic and so is the primordial power spectrum. On the other hand, for $c > 1$ one finds the nontrivial attractor solution for the electric field and the anisotropic metric of the form (3). The deviation from the rotational invariance is measured by [7,26]

$$\frac{\Sigma}{H} = \frac{1}{3}\frac{c-1}{c}\epsilon, \quad (6)$$

where ϵ is the slow-roll parameter. The amplitude of statistical anisotropy is related to the violation of rotational invariance, i.e., $g_* \propto \Sigma/H$.

In fact, even for the case $c = 1$, one finds the anisotropic power spectrum [11]. This is due to the enhancement of the infrared fluctuations of the gauge field by the standard inflationary mechanism. These quantum fluctuations behave like the classical field after they exit the horizon. Consequently, modes which exit the horizon before the time $N_{\rm CMB} \approx 60$ in the number of e-folds act as an additional anisotropic background for inflaton fluctuations. To account for this new effect (pointed out in Ref. [11]), one should study the evolution of inflaton fluctuations in the overall classical electric field,

$$\mathbf{E}_{\rm cl} = \mathbf{E}_0 + \mathbf{E}_{\rm IR}.$$

Here $\mathbf{E}_0$ follows from the equation of motion (e.o.m.), while $\mathbf{E}_{\rm IR}$ originates from quantum fluctuations, which get enhanced and classicalize before the time $N_{\rm CMB}$ when inflaton perturbations leave the horizon (hence the subscript "IR"). Note that $\mathbf{E}_{\rm IR}$ is a random Gaussian field characterized by zero mean and variance [11],

$$\langle \mathbf{E}_{\rm IR}^2\rangle = \frac{9H^4}{2\pi^2}N. \quad (7)$$

Here N is the number of e-folds from the beginning of inflation until the time $N_{\rm CMB}$, i.e., $N = N_{\rm tot} - N_{\rm CMB}$, with $N_{\rm tot}$ being the overall number of e-folds during inflation.

Taking into account both sources of statistical anisotropy, one writes the amplitude g_* as follows [11]:

$$g_* = -\frac{24}{\epsilon}\cdot\frac{E_{\rm cl}^2}{V(\phi)}\cdot N_{\rm CMB}^2. \quad (8)$$

(See also Ref. [12].) Quite unexpectedly, one observes a large magnitude of statistical anisotropy [7,11]. So, the order-one amplitude $g_* = \mathcal{O}(1)$ is obtained already for the ratio ρ_A/V as tiny as $\mathcal{O}(10^{-5})$. The point is that one expects a much larger energy density ρ_A on rather general grounds. Indeed, according to its quantum origin, we note that the

[1] Upon substituting the first relation of Eq. (5) into Eq. (1), we obtain the power spectrum $\mathcal{P}_\zeta(\mathbf{k}) = \mathcal{P}_\zeta(k)(1 + g_*\cos^2\theta - 1/3\cdot g_*)$, which is somewhat different from the one given by Eq. (4). The difference, however, is the direction-independent piece, which can be absorbed into the redefinition of the spectrum $\mathcal{P}_\zeta(k)$.

factor N in Eq. (7) is considered to be a large number in conventional inflationary scenarios, which gives rise to the naturally large amplitude g_*. To handle the situation, one assumes a tuned duration of inflation, i.e., $N_{\rm tot} \sim N_{\rm CMB}$. We reiterate this statement in the future, when imposing constraints on model parameters. Furthermore, the purely classical field $\mathbf{E}_0$ is related to the potential $V(\phi)$ by

$$E_0^2 = \frac{c-1}{c} V(\phi)\epsilon. \tag{9}$$

Substituting this into Eq. (8), one observes that one needs an extremely tuned value of the constant c. Namely, the order-one amplitude g_* is obtained provided that $c - 1 \sim 10^{-5}$.

To summarize, the special quadrupole predicted in the anisotropic inflation has a twofold origin, which translates into the twofold treatment of the amplitude g_*. If the purely classical effect is most relevant, the quantity g_* is directly related to the intrinsic parameters of the model. There is no direct matching provided that the amplitude g_* is sourced by the random field $\mathbf{E}_{\rm IR}$. Barring fine-tuning, we focus on these two situations in what follows:

(I) $E_0 \gg E_{\rm IR}$, and, consequently, $E_{\rm cl} \to E_0$ is achieved in the formal limit $N_{\rm tot} \to N_{\rm CMB}$. In this case, by substituting Eq. (9) into Eq. (8) we obtain for the amplitude

$$g_* = -24 \cdot \frac{c-1}{c} \cdot N_{\rm CMB}^2. \tag{10}$$

(II) $E_0 \ll E_{\rm IR}$, and, consequently, $E_{\rm cl} \to E_{\rm IR}$, which occurs for $c \to 1$.

We write the corresponding amplitude as follows:

$$g_* = -\mathbf{a}^2, \qquad \mathbf{a} = 24 \cdot \Delta_\zeta \cdot N_{\rm CMB} \cdot \frac{\mathbf{E}_{\rm IR}}{\sqrt{2\langle E_{\rm IR}^2\rangle_1}}, \tag{11}$$

where we make use of the slow-roll relations

$$H^2 = \frac{8\pi}{3M_{\rm Pl}^2} V(\phi), \qquad \Delta_\zeta \equiv \sqrt{\mathcal{P}_\zeta} = \sqrt{\frac{H^4}{4\pi^2\dot\phi^2}}, \qquad \frac{\dot\phi^2}{2V} = \frac{\epsilon}{3}.$$

The subscript "1" denotes the quantity $\langle \mathbf{E}_{\rm IR}^2 \rangle$ formally calculated for the total number of e-folds $N_{\rm tot} = N_{\rm CMB} + 1$. The convenience of the vector $\mathbf{a}$ introduced in Eq. (11) is that its components a_i obey Gaussian statistics (unlike the amplitude g_*). Namely, they have zero means and variances given by

$$\langle \mathbf{a}_i^2 \rangle = 96 \cdot \mathcal{P}_\zeta \cdot N_{\rm CMB}^2 \cdot N. \tag{12}$$

Considering the cases I and II separately is natural, since the fields E_0 and $E_{\rm IR}$ are largely unrelated to each other barring scenarios where two electric fields accidentally cancel each other with a high accuracy. With this qualification case I results in the constraint on the parameter c, while case II leads to an upper limit on the duration of inflation.

Equations (5), (10), and (12) will be the starting point of our discussion in Sec. V, when constraining anisotropic inflation.

III. THE (PSEUDO)CONFORMAL UNIVERSE

Generating statistical anisotropy at inflation requires strong assumptions about the inflationary stage, at least in the model we have discussed. On the other hand, a violation of statistical isotropy may arise naturally in alternative frameworks, e.g., the (pseudo)conformal universe. In Secs. III A and III B, we briefly summarize some basic features inherent to this cosmological picture, while referring to Refs. [13–15] for detailed discussions. Predictions for statistical anisotropy are reviewed in Secs. III C and III D.

A. Basic assumptions and the scale-invariant power spectrum

In the (pseudo)conformal universe, the observed flatness of the primordial power spectrum is due to conformal symmetry at very early stages of the Universe. In more detail, there are several conditions to be satisfied [15]:

(i) The space-time is described by the nearly Minkowski metric at very early times.
(ii) The matter in the Universe is in the conformal field theory state.
(iii) Among the field contents of the Universe there are at least two scalars: one with the conformal weight $\Delta \neq 0$ and another with the weight $\Delta = 0$.
(iv) Classical equations of motion admit the nontrivial time-dependent solution of the field with $\Delta \neq 0$.
(v) The action is invariant under the shift of the weight-0 field, $\sigma \to \sigma + c$.

Given these conditions, weight-0 field perturbations evolving in the background created by the $\Delta \neq 0$ conformal field acquire a scale-invariant power spectrum. On the other hand, relaxing one or more of the above conditions may lead to the small scalar tilt [15,27], as required by the experimental data [28].

Specifying to known realizations of the (pseudo)conformal universe, we choose the nonzero conformal weight to be equal to 1. Then, the generic action of the (pseudo) conformal universe can be written in the form

$$S = S_{\rm G+M} + S_\rho + \frac{1}{2}\int d^4x\sqrt{-g}\rho^2(\partial\sigma)^2, \tag{13}$$

where $S_{\rm G+M}$ is the action for gravity and some matter preexisting in the early Universe. The third term on the r.h.s. describes the minimal conformal coupling of the weight-0

field σ to the field ρ, while the second term encodes the dynamics of the field ρ, which it has on its own. By assumption, the action S_ρ allows for the classical solution of the field ρ given by Eq. (2), where the time dependence is fixed by conformal invariance. We recall that the parameter h entering Eq. (2) is the dimensionless constant originating from the action S_ρ, while t_* is an arbitrary constant of integration which has the meaning of the end-of-roll time.

The solution (2) spontaneously breaks the conformal group SO(4,2) down to the de Sitter subgroup SO(4,1) [15]. Interestingly, this symmetry-breaking pattern uniquely determines the phenomenological properties of perturbations of the field σ. Namely, independently of the details of the microscopic physics, the field σ acquires the power spectrum of the Harrison-Zel'dovich type [15]. To show this explicitly, one introduces the notation $\chi = \rho_0 \delta\sigma$. From Eq. (13), one derives the e.o.m. for the field χ,

$$\ddot{\chi} - \partial_i \partial_i \chi - 2h^2 \rho_0^2 \chi = 0. \tag{14}$$

(The unit scale factor $a = 1$ is assumed here). We observe that with the classical background ρ_0 as in Eq. (2), the e.o.m. (14) coincides with that of the massless scalar field in the de Sitter background. Hence, the result is the same, namely, a scale-invariant power spectrum which reads in terms of σ perturbations [13–15]

$$\mathcal{P}_{\delta\sigma} = \frac{h^2}{4\pi^2}.$$

We reiterate that the scale invariance as well as the results summarized in the next subsections are largely independent of the details of the microscopic physics. So far, two concrete models have been proposed. These are the conformal rolling scenario [13] and Galilean genesis [14].

The former represents perhaps the simplest realization of the (pseudo)conformal universe. There the field ρ is a scalar with the standard kinetic term rolling down the negative quartic potential. The action for this rolling field is given by [13]

$$S_\rho = \int d^4x \sqrt{-g}[(\partial\rho)^2 + h^2\rho^4]. \tag{15}$$

It is straightforward to show that the classical field ρ has an attractor solution given by Eq. (2). The conformal rolling scenario is natural from both the dynamical and spectator prospectives. In the former situation, the Universe driven by the field ρ undergoes a slow contraction [15] akin to ekpyrotic scenarios [29]. Alternatively, one treats the field ρ as a spectator. In that case, the Minkowski metric can be imposed "by hand." The other possibility discussed in the original proposal of the conformal rolling scenario [13] is to conformally couple the spectator field ρ to gravity. The background evolution of the Universe is then allowed to be arbitrary during the conformal phase. In what follows, we assume the minimal coupling to gravity with minimal loss of generality.

Galilean genesis is the other example of a (pseudo) conformal universe model [14]. Its action is given by

$$S_\pi = \int d^4x \sqrt{-g}\left[-f^2 e^{2\pi}(\partial\pi)^2 + \frac{f^3}{\Lambda_G^3}(\partial\pi)^2\Box\pi + \frac{f^3}{2\Lambda_G^3}(\partial\pi)^4\right],$$

where the field π, the Galileon, is defined by $\rho = f e^\pi$. Despite the higher-derivative structure of the Galilean genesis action, the e.o.m. is second order in derivatives of the field π. Moreover, the e.o.m. admits a solution of the form (2). In fact, the correspondence between Galilean genesis and the conformal rolling scenario is much deeper: the predictions of the two models are the same modulo the replacement

$$h^2 \leftrightarrow \frac{2}{3}\frac{\Lambda_G^3}{f^3}. \tag{16}$$

Note that the Galileon π is naturally treated as a dynamical field. Driven by the field π, the Universe is nearly static at very early times, but slowly expands. Thus, the first condition outlined in the beginning of this section is satisfied automatically, at least at early times.

B. Weight-0 perturbations: next-to-leading order

The interaction between weight-0 and weight-1 field perturbations sources nontrivial phenomenology in (pseudo)conformal universe models [16–18,30]. In particular, it gives rise to some amount of statistical anisotropy.

Perturbations of the field ρ have a red power spectrum whose form is fixed by the symmetry-breaking pattern $\mathrm{SO}(4,2) \to \mathrm{SO}(4,1)$. As discussed in Refs. [13–16], they can be absorbed into the redefinition of the end-of-roll time t_*, i.e.,

$$\rho \propto \frac{1}{t_*(\mathbf{x}) - t}. \tag{17}$$

Here

$$t_*(\mathbf{x}) = t_* + \delta t_*(\mathbf{x}),$$

and the shift of time $\delta t_*(\mathbf{x})$ is the random field with the red power spectrum

$$\langle \delta t_*^2(\mathbf{x}) \rangle \propto h^2 \int \frac{dp}{p^2},$$

where $p = |\mathbf{p}|$ are wave numbers characterizing the Fourier modes of the field ρ. Clearly, the shift δt_* as it stands is irrelevant from the physical point of view, since it can be absorbed into the redefinition of the end-of-roll time t_*. Interesting effects appear once we consider the spatial variation of $t_*(\mathbf{x})$. It is convenient to introduce the notation

$$v_i = -\partial_i t_*(\mathbf{x}),$$

while keeping the standard notation for the second derivative, i.e., $\partial_i\partial_j t_*$. The field $\mathbf{v}$ is a random Gaussian field with zero mean and variance,

$$\langle v_i^2\rangle = \frac{3h^2}{8\pi^2}\,\ln\frac{H_0}{\Lambda}. \tag{18}$$

Here H_0 is the present Hubble rate; Λ is an infrared cutoff. To account for the interaction with long-ranged radial perturbations, one studies the evolution of weight-0 perturbations in the inhomogeneous background (17). This calculation was done in Ref. [16] including corrections of the orders $\partial_i\partial_j t_*/k$ and v^2. The result for the perturbations $\delta\sigma$ in the late-time regime $k(t_* - t) \ll 1$ is

$$\delta\sigma(\mathbf{x},\eta) = \int \frac{d^3k}{\sqrt{k}}\frac{h}{4\pi^{3/2}\gamma(k+\mathbf{kv})} \times e^{i\mathbf{kx}-ikt_*(\mathbf{x})}\left(1-\frac{\pi}{2k}\frac{k_ik_j}{k^2}\partial_i\partial_j t_* + \frac{\pi}{6k}\partial_i\partial_i t_*\right)A_{\mathbf{k}} + \text{H.c.} \tag{19}$$

Here $\gamma = (1-v^2)^{-1/2}$, and the expansion to order v^2 is understood; $A_{\mathbf{k}}$ is the annihilation operator for the perturbations $\delta\sigma$. Note that perturbations of the weight-0 field σ remain frozen out until the end of conformal rolling.

After conformal symmetries get broken, the form of the solution (19) is no longer protected. Still, there is the option that cosmological modes of interest are already superhorizon at this time, and the perturbations $\delta\sigma$ remain unchanged until the RD stage. In the nomenclature of Ref. [19], this is "sub-scenario A." Note that sub-scenario A is natural from both the dynamical and spectator prospectives. Alternatively, the cosmological perturbations $\delta\sigma$ may be subhorizon by the end of the roll. In that case, the perturbations $\delta\sigma$ evolve before the beginning of the hot era. This option is not particularly natural in dynamical models, but can be well accommodated in spectator versions of the (pseudo)conformal universe. We call this option "sub-scenario B."

The two sub-scenarios lead to drastically different predictions for statistical anisotropy, as we discuss below.

C. Sub-scenario A

In sub-scenario A, the primordial power spectrum of scalar perturbations is derived directly from Eq. (19). For reasons which will become clear shortly, we write it up to the quadratic order in the constant h,

$$\mathcal{P}_\zeta(\mathbf{k}) = \mathcal{P}_\zeta(k)[1 + Q_1(\mathbf{k}) + Q_2(\mathbf{k})]. \tag{20}$$

Here $Q_1(\mathbf{k})$ is the leading-order contribution, which is already nonzero at the linear order in h [16,18],

$$Q_1(\mathbf{k}) = -\frac{\pi}{k}\hat{k}_i\hat{k}_j\partial_i\partial_j t_*. \tag{21}$$

This encodes a statistical anisotropy of the general quadrupole type in contrast to the inflationary predictions of Sec. II. The third term in the square brackets in Eq. (20) is given by [16,18]

$$Q_2(\mathbf{k}) = -\frac{3}{2}v_iv_j\hat{k}_i\hat{k}_j. \tag{22}$$

The direction dependence present here is of the special quadrupole type akin to inflation with vector fields. Note its quadratic dependence on the "velocity," which implies the suppression by the additional power of the constant h as compared to the contribution (21). This, however, does not mean that the special quadrupole can be ignored in the data analysis. Moreover, if the constant h is not particularly small, the term (22) effectively makes a larger imprint on the CMB sky than the general quadrupole with the amplitude decreasing as k^{-1}. At the level of cosmological measurements, the latter property translates into the suppression at large CMB multipole number $l \propto H_0k^{-1}$. As a result, we have low statistics for the multipoles that are relevant in this analysis, and hence a very weak constraint on the parameter h from the nonobservation of the general quadrupole [19]. We will return to this discussion in Sec. V, when constraining sub-scenario A.

Let us rewrite Eq. (21) in the conventional form,

$$Q_1(\mathbf{k}) = a(k)\sum_M q_{2M}Y_{2M}(\hat{\mathbf{k}}). \tag{23}$$

Here q_{2M} are random Gaussian quantities with zero means and variances,

$$\langle q_{2M}q^*_{2M'}\rangle = \frac{\pi h^2}{25}\delta_{MM'}, \tag{24}$$

while the direction-independent amplitude $a(k)$ is given by

$$a(k) = H_0k^{-1}. \tag{25}$$

On the other hand, the special quadrupole corresponding to the subleading-order statistical anisotropy is characterized by the scale-independent amplitude

$$g_* = -\frac{3}{2}v^2, \tag{26}$$

and the preferred direction is associated with the unit random vector $\hat{\mathbf{v}} = \mathbf{v}/v$. Remarkably, this prediction is very similar to the statistical anisotropy following from case II of anisotropic inflation, sourced by the Gaussian random vector $\mathbf{E}_{\text{IR}}$. Formally equating the amplitudes (11) and (26), and using Eqs. (12) and (18), we conclude that the duality holds up to the replacement

$$h^2 \ln\frac{H_0}{\Lambda} \leftrightarrow \frac{512\pi^2}{3}\mathcal{P}_\zeta N_{\rm CMB}^2 N. \tag{27}$$

We exploit this duality when constraining sub-scenario A in Sec. V.

D. Sub-scenario B

If cosmological modes are subhorizon by the end of the roll, they proceed to evolve at the so-called intermediate stage [17] which ends as modes of interest leave the horizon. In the conformal rolling scenario, the end of the roll is realized by relaxing the form of the potential in Eq. (15), so that it has a minimum at some large field value $\rho = f$. After the field ρ reaches its minimum, the field σ evolves as the massless scalar minimally coupled to gravity. We claim that the evolution during the intermediate stage is long enough, i.e., $r \equiv t_1 - t_* \gg k^{-1}$, where t_1 is the time when the perturbations $\delta\sigma$ get frozen out (in the conventional sense). Second, cosmological evolution at the intermediate stage must be described by the nearly Minkowski metric. Otherwise, the flat spectrum of perturbations generated by the end of the conformal phase would be grossly modified. With these assumptions, the dynamics at the intermediate stage is fairly nontrivial, and the final expression for the perturbations $\delta\sigma$ is quite complicated. Here we simply write down the result for the power spectrum of primordial scalar perturbations [17],

$$\mathcal{P}_\zeta(\mathbf{k}) = \mathcal{P}_\zeta(k)[1 + \mathbf{n}_k(\mathbf{v}(\mathbf{n}_k r) - \mathbf{v}(-\mathbf{n}_k r))].$$

Remarkably, the direction dependence present here is nonzero already at the linear order in the constant h. Moreover, it encodes the statistical anisotropy of all even multipoles starting from the quadrupole of the general type, i.e., all the coefficients q_{LM} with even L are nonzero in Eq. (1). They are random Gaussian variables with zero means and variances given by [17]

$$\langle q_{LM} q^*_{L'M'}\rangle \equiv Q_L \delta_{LL'}\delta_{MM'} = \frac{3}{\pi}\frac{h^2}{(L-1)(L+2)}\delta_{LL'}\delta_{MM'}. \tag{28}$$

Remarkably, the amplitude $a(k)$ does not depend on the wave number k, i.e., $a(k) = 1$.

The prediction of sub-scenario B for statistical anisotropy is in sharp contrast to that of inflationary scenarios.

IV. ESTIMATORS

As the first step, we discuss estimators for the amplitudes q_{LM} entering the primordial power spectrum (1). Following Ref. [20], we make use of the QML methodology. This technique was argued to be in good agreement with the exact likelihood methods applied to the search for the statistical anisotropy with the WMAP5 data [21,22]. In our previous paper, we applied QML-based estimators to the 7-year release of the WMAP data and constrained the conformal rolling scenario from the nonobservation of statistical anisotropy.

Let us recall the main ideas behind the QML estimator. One starts with the log-likelihood $\mathcal{L}$ of the observed sky $\hat{\mathbf{\Theta}}$ with respect to the coefficients q_{LM} of statistical anisotropy. Assuming that these parameters are small enough, one expands the log-likelihood up to the quadratic order in the q_{LM}'s,

$$\mathcal{L}(\hat{\mathbf{\Theta}}|\mathbf{q}) = \mathcal{L}_0 + \mathbf{q}^\dagger \left.\frac{\partial\mathcal{L}}{\partial\mathbf{q}^\dagger}\right|_0 + \frac{1}{2}\mathbf{q}^\dagger \left\langle\frac{\partial^2\mathcal{L}}{\partial\mathbf{q}^\dagger\partial\mathbf{q}}\right\rangle\Bigg|_0 \mathbf{q}, \tag{29}$$

where the subscript "0" denotes that corresponding quantities are calculated in the absence of statistical anisotropy. In Eq. (29) we replaced the second derivative of the log-likelihood by its expectation value. The QML estimator for $\mathbf{q}$ is obtained by setting the derivative of the quadratic log-likelihood to zero with respect to $\mathbf{q}^\dagger$,

$$\mathbf{q} = \mathbf{F}^{-1}\left.\frac{\partial\mathcal{L}}{\partial\mathbf{q}^\dagger}\right|_0. \tag{30}$$

Here $\mathbf{F}$ is the Fisher matrix defined as

$$\mathbf{F} \equiv \left\langle\frac{\partial\mathcal{L}}{\partial\mathbf{q}}\frac{\partial\mathcal{L}}{\partial\mathbf{q}^\dagger}\right\rangle\Bigg|_0 = -\left\langle\frac{\partial^2\mathcal{L}}{\partial\mathbf{q}^\dagger\partial\mathbf{q}}\right\rangle\Bigg|_0.$$

The equality here follows from the normalization condition for the likelihood.

To concretize the form of the estimator, we assume Gaussian temperature fluctuations. The log-likelihood then reads

$$-\mathcal{L}(\hat{\mathbf{\Theta}}|\mathbf{q})|_0 = \frac{1}{2}\hat{\mathbf{\Theta}}^\dagger\mathbf{C}^{-1}\hat{\mathbf{\Theta}} + \frac{1}{2}\ln\det\mathbf{C}, \tag{31}$$

where $\mathbf{C}$ denotes the covariance matrix incorporating the theoretical covariance as well as the instrumental noise, $\mathbf{C} = \mathbf{S} + \mathbf{N}$. The first derivative of the log-likelihood (31) is given by

$$\frac{\partial\mathcal{L}}{\partial\mathbf{q}^\dagger} = \frac{1}{2}\bar{\mathbf{\Theta}}^\dagger\frac{\partial\mathbf{C}}{\partial\mathbf{q}^\dagger}\bar{\mathbf{\Theta}} - \frac{1}{2}\left\langle\bar{\mathbf{\Theta}}^\dagger\frac{\partial\mathbf{C}}{\partial\mathbf{q}^\dagger}\bar{\mathbf{\Theta}}\right\rangle. \tag{32}$$

The vector $\bar{\mathbf{\Theta}}$ represents the collection of CMB temperature coefficients filtered with the inverse isotropic covariance,

$$\bar{\mathbf{\Theta}} = (\mathbf{S}^i + \mathbf{N})^{-1}\hat{\mathbf{\Theta}}. \tag{33}$$

Here $\mathbf{S}^i$ is the theoretical covariance calculated in the absence of statistical anisotropy,

$$S^{i}_{lm;l'm'} = C_l \delta_{ll'} \delta_{mm'}, \tag{34}$$

with the C_l's representing the standard angular power spectrum. The derivative of the covariance with respect to the coefficients q^*_{LM} is given by

$$\frac{\partial C_{lm;l'm'}}{\partial q^*_{LM}} = i^{l'-l} C_{ll'} \int d\Omega_{\mathbf{k}} Y^*_{lm}(\hat{\mathbf{k}}) Y_{l'm'}(\hat{\mathbf{k}}) Y^*_{LM}(\hat{\mathbf{k}}), \tag{35}$$

where

$$C_{ll'} = 4\pi \int d\, \ln k \Delta_l(k) \Delta_{l'}(k) a(k) \mathcal{P}_\zeta(k), \tag{36}$$

and $\Delta_l(k)$ is a transfer function. For the particular case of $l = l'$ and a constant amplitude $a(k) = 1$, the coefficients $C_{ll'}$ reduce to the angular power spectrum C_l. Equation (35) follows from the expression for the theoretical covariance $\mathbf{S}$ which we write here for future reference,

$$S_{lm;l'm'} = 4\pi i^{l'-l} \int \frac{d\mathbf{k}}{k^3} Y^*_{lm}(\hat{\mathbf{k}}) Y_{l'm'}(\hat{\mathbf{k}}) \Delta_l(k) \Delta_{l'}(k) \mathcal{P}_\zeta(\mathbf{k}). \tag{37}$$

It takes the diagonal form (34) for a statistically isotropic power spectrum $\mathcal{P}_\zeta(\mathbf{k}) = \mathcal{P}_\zeta(k)$.

The straightforward way to evaluate the Fisher matrix entering Eq. (30) is to average the product of two log-likelihood derivatives over the large number of statistically isotropic Monte Carlo (MC) maps. A good forecast, however, is given in terms of the analytic Fisher matrix calculated in the homogeneous noise approximation. Only diagonal elements of the Fisher matrix survive in that case, i.e.,

$$\begin{aligned} F_{LM;L'M'} &\equiv F_L \delta_{LL'} \delta_{MM'} \\ &= \delta_{LL'} \delta_{MM'} f_{\rm sky} \sum_{l,l'} \frac{(2l+1)(2l'+1)}{8\pi} \\ &\quad \times \begin{pmatrix} L & l & l' \\ 0 & 0 & 0 \end{pmatrix}^2 \frac{C^2_{ll'}}{C^{\rm tot}_l C^{\rm tot}_{l'}}, \end{aligned} \tag{38}$$

where $C^{\rm tot}_l = C_l + N_l$; the prefactor $f_{\rm sky}$ is an unmasked fraction of the sky. The formula (38) completes the derivation of the estimators for the coefficients q_{LM}. Out of the amplitudes q_{LM}, one further reconstructs the coefficients C^q_L defined in the standard manner,

$$C^q_L = \frac{1}{2L+1} \sum_M |q_{LM}|^2. \tag{39}$$

These can be used to test the CMB statistical anisotropy in a model-independent way.

A. Statistical anisotropy of the special quadrupole type with constant amplitude

To constrain the statistical anisotropy of the special quadrupole type, we slightly modify the above procedure. Our first goal is to construct the estimator for the amplitude g_* given some fixed preferred direction $\mathbf{d}$. For this purpose, we consider the log-likelihood as the function of the unique parameter g_*, i.e., $\mathcal{L}(\hat{\mathbf{\Theta}}|g_*)$. Then, following the same steps outlined above, we obtain

$$g_* = \frac{3}{2} \cdot {\rm Re}\left(\sum_M q_{2M} Y_{2M}(\mathbf{d}) \right). \tag{40}$$

So, the estimate for the amplitude g_* is reproduced immediately from estimates for the coefficients q_{2M}. Furthermore, the estimator (40) is unbiased and has a minimal variance.

Recall that the early Universe models generically do not predict the preferred direction of statistical anisotropy. To estimate the amplitude g_* in a universal way, we exploit the second relation in Eq. (5),

$$g^2_* = \frac{45}{16\pi} \sum_M |q_{2M}|^2 \equiv \frac{225}{16\pi} C^q_2. \tag{41}$$

Though this estimator has an intuitively clear form, it is "blind" to the sign of the amplitude g_*. The other disadvantage of the estimator (41) is that it does not discriminate between the special and general types of quadrupoles. Consequently, we expect somewhat weaker constraints than in the case with the specified preferred direction. This is the price we pay for our ignorance about the latter.

B. Statistical anisotropy of the general type with Gaussian q_{LM}'s

Generically, statistical anisotropy is described by the infinite number of *random* parameters q_{LM}. First, we treat the case of Gaussian coefficients q_{LM} as in sub-scenario B of the (pseudo)conformal universe. In this situation, the likelihood of the observed sky $\hat{\mathbf{\Theta}}$ is naturally considered as a function of the parameter h^2. The corresponding estimator was derived in our previous paper [19]. Let us briefly recall the main idea of the calculation. We write the likelihood of interest as the product of two likelihoods integrated over all possible sets of coefficients $\{q_{LM}\}$, i.e.,

$$\mathcal{W}(\hat{\mathbf{\Theta}}|h^2) = \int \mathcal{W}(\hat{\mathbf{\Theta}}|\mathbf{q}) \mathcal{W}(\mathbf{q}|h^2) d\mathbf{q}. \tag{42}$$

Here $\mathcal{W}(\hat{\mathbf{\Theta}}|\mathbf{q}) = \exp(\mathcal{L})$, and $\mathcal{L}$ is given by Eq. (31); $\mathcal{W}(\mathbf{q}|h^2)$ denotes the likelihood of the particular realization $\mathbf{q}$ for a given value of the parameter h^2. Upon using the approximation (29), we obtain the simple Gaussian form

for the integrand in Eq. (42). Then the integral (42) is evaluated in a straightforward manner. Finally, setting the derivative of the joint likelihood with respect to the parameter h^2 to zero, we end up with the estimator [19]

$$h^2\sum_L \frac{(2L+1)F_L^2\tilde{Q}_L^2}{(1+F_L\tilde{Q}_L h^2)^2}=\sum_L \frac{(2L+1)F_L\tilde{Q}_L}{(1+F_L\tilde{Q}_L h^2)^2}(F_L C_L^q-1). \tag{43}$$

Here the $\tilde{Q}_L$'s are defined by $Q_L=\tilde{Q}_L h^2$, and the Q_L's are given by Eq. (28). The estimator (43) is simplified considerably in the case of the quadrupole statistical anisotropy with the Gaussian q_{2M}'s,

$$h^2 \simeq C_2^q - F_2^{-1}, \tag{44}$$

where we omitted the irrelevant constant prefactor. We exploit this estimator in Sec. V when constraining the quadrupole of the general type predicted in the leading order of sub-scenario A of the (pseudo)conformal universe.

Finally, let us discuss estimators for statistical anisotropy of the special quadrupole type governed by the *non-Gaussian* amplitude g_*. This type of direction dependence, we recall, arises in sub-scenario A of the (pseudo)conformal universe (in the subleading order) as well as in anisotropic inflation (case II). In that case, the discussion above is not applicable. Still, at the price of optimality, we choose to work with simple quadratic estimators built of estimators for the coefficients q_{2M}. Namely,

$$N^2, \qquad h^4 \ln^2\frac{H_0}{\Lambda} \simeq C_2^q. \tag{45}$$

V. DATA ANALYSIS AND RESULTS

In the present section, we constrain early Universe models by applying the estimators (40), (41), (43), (44), and (45) to the WMAP9 data. The 9-year data set includes a new product: a set of beam-symmetrized maps, produced by a deconvolution procedure to eliminate the effects of the asymmetric beam [25]. The latter effects were responsible for the strong bias in the measurements of the statistical anisotropy [24]. One may treat the deconvolved map as a map measured by a hypothetical WMAP-like satellite with a symmetric beam transfer function. Therefore, a simple relation between real and observed signals is assumed in deconvolved maps,

$$\hat{\Theta}_{lm}=B_l\Theta_{lm}+N_{lm}, \tag{46}$$

where B_l is a symmetric part of the beam transfer function and N_{lm} is a noise. The same relation was used in the previous analyses [19,20]. With this said, we can estimate the coefficients q_{LM} and C_L^q literally following the techniques in Ref. [20]. The first and most costly step here is to provide the inverse-variance filtering (33). For the purpose of the numerical computations, we rewrite Eq. (33) in the equivalent form

$$[(\mathbf{S}^i)^{-1}+\tilde{\mathbf{Y}}^\dagger\mathbf{N}^{-1}\tilde{\mathbf{Y}}]\mathbf{S}^i\bar{\mathbf{\Theta}}=\tilde{\mathbf{Y}}^\dagger\mathbf{N}^{-1}\hat{\mathbf{\Theta}}. \tag{47}$$

Here $\tilde{\mathbf{Y}}$ is a matrix which relates the harmonic space covariance and the observed map,

$$\tilde{Y}_{ilm}=B_l Y_{lm}(i).$$

To solve the system (47), we make use of the multigrid preconditioner proposed in Ref. [31]. Having inversed filtered temperature anisotropies for both real data and a large number of MC maps, we evaluate estimators for the coefficients q_{LM} by using Eq. (30) and substituting Eqs. (32), (35), (36), and (38). We compute the integral over three spherical harmonics in Eq. (35) using the Slatec [32] and GSL [33] libraries, and the coefficients $C_{ll'}$ by running CAMB [34]. The summation over the multipole number l in Eq. (32) is performed up to $l_{\max}=400$. The second term in Eq. (32) is calculated by averaging over the large number of MC maps. We evaluate the Fisher matrix using the analytical expression (38). The WMAP9 *kq85* temperature analysis mask is applied to both data and MC maps leaving $f_{\rm sky}=75\%$ of the sky unmasked.

In Fig. 1, we present the coefficients C_L^q reconstructed from the *V* and *W* bands of the WMAP9 maps. As is clearly seen, WMAP9 data favor statistically isotropic primordial perturbations. This is to be compared with the analogous results from the 5- and 7-year releases revealing the anomalously large quadrupole [20–22]. Now, given the absence of the anomaly, we expect a substantial tightening of constraints on the early Universe models.

A. Constraints on anisotropic inflation

We start with constraining the amplitude g_* of the quadrupole of the special type. This is interesting from the viewpoint of scenarios where g_* is uniquely defined by the model parameters, as in case I of anisotropic inflation. First, we apply the estimator (40) in order to constrain the amplitude for some particular preferred directions. The results of the estimation are presented in Fig. 2. The constraining procedure is as follows:

(i) We calculate the set $\{q_{2M}\}=q_{2,-2},q_{2,-1},\ldots,q_{2,2}$ starting from some fixed value of g_* and preferred direction $\mathbf{d}$.

(ii) For the set $\{q_{2M}\}$, we generate a number of anisotropic maps and estimate the amplitude g_* from the latter. We make use of Eq. (40).

(iii) We compare the values of g_* derived from anisotropic maps with the WMAP9 estimate. We request that not more than 95% of them exceed (are smaller than) the real estimate in the case of positive (negative) g_* fixed in the beginning.

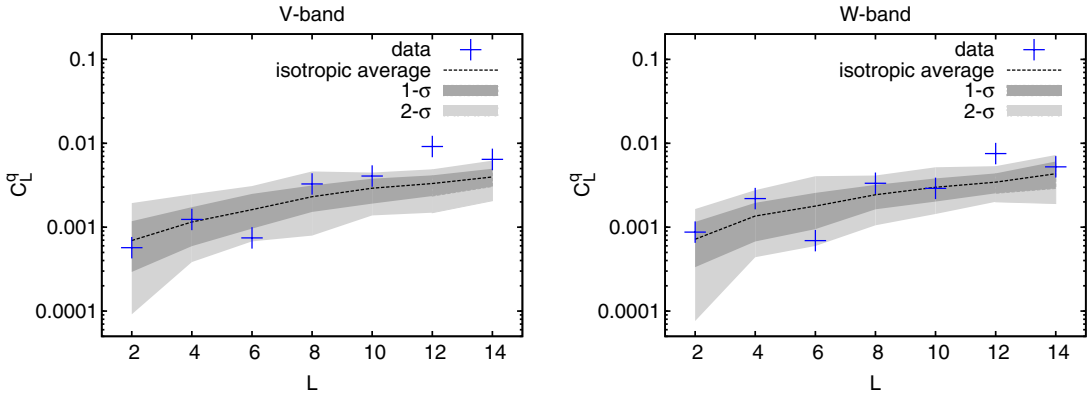

FIG. 1 (color online). The coefficients C_L^q reconstructed from the V (left) and W (right) bands of deconvolved WMAP9 maps in the case of $a(k) = 1$ in Eq. (1). The 1σ (dark grey) and 2σ (light grey) confidence levels are overlaid by making use of MC-generated statistically isotropic maps. The analysis is done with the WMAP9 temperature analysis mask and $l_{\max} = 400$.

The generation of anisotropic maps is perhaps the most nontrivial step in this procedure. We do this in line with Appendix A of Ref. [20] (see also our previous paper [19]). The idea is to consider the temperature anisotropy of the form

$$\mathbf{\Theta}^a = (\mathbf{I} + \delta\mathbf{S}[\mathbf{S}^i]^{-1}])^{1/2}\mathbf{\Theta}^i, \tag{48}$$

where $\delta\mathbf{S} \equiv \mathbf{S} - \mathbf{S}^i$. Here $\mathbf{S}$ and $\mathbf{S}^i$ are the anisotropic and isotropic theoretical covariances given by Eqs. (37) and (34), respectively. It is straightforward to check that the temperature anisotropy (48) corresponds to the anisotropic covariance $\mathbf{S}$. Assuming a small statistical anisotropy, we expand it to the linear order in $\delta\mathbf{S}$,

$$\mathbf{\Theta}^a = \mathbf{\Theta}^i + \frac{1}{2}\delta\mathbf{S}[\mathbf{S}^i]\mathbf{\Theta}^i.$$

We multiply the latter by the symmetric beam, convert into the pixel space, add the noise, and apply the mask. The anisotropic maps constructed are then analyzed in the same way as the data maps. We followed the above procedure for the three fixed directions in the sky. The directions form an orthogonal basis with the first one aligned with the poles of the ecliptic plane. Constraints on the amplitude g_* are presented in Table I. We also establish 68% C.L. limits in the case of the direction aligned with the ecliptic poles,

$$-0.018 < g_* < 0.021. \tag{49}$$

These limits are obtained from the V band of the WMAP9 data. They are to be compared with the analogous constraints derived from the nonobservation of quadrupolar statistical anisotropy in the data by the Sloan Digital Sky Survey which found $g_* = 0.006 \pm 0.036$ at 68% C.L. [23]. As is clearly seen, our bounds are consistent with previous ones but demonstrate an improvement by a factor of 2.

Aiming to limit the amplitude g_* without knowledge of the preferred direction, we repeat the above procedure with minor changes. That is, we choose about 100 random directions in the sky and calculate sets $\{q_{2M}\}$ using Eq. (5). For each set $\{q_{2M}\}$, we generate an anisotropic map. Now, we employ Eq. (41) to estimate the strength of statistical anisotropy in real data as well as in simulated anisotropic maps. In fact, we construct MC maps for concrete directions, but the procedure requires that the data and MC maps are treated on an equal footing. The results are presented in Table II. They demonstrate a substantial improvement as compared to the WMAP5 constraints, which are also

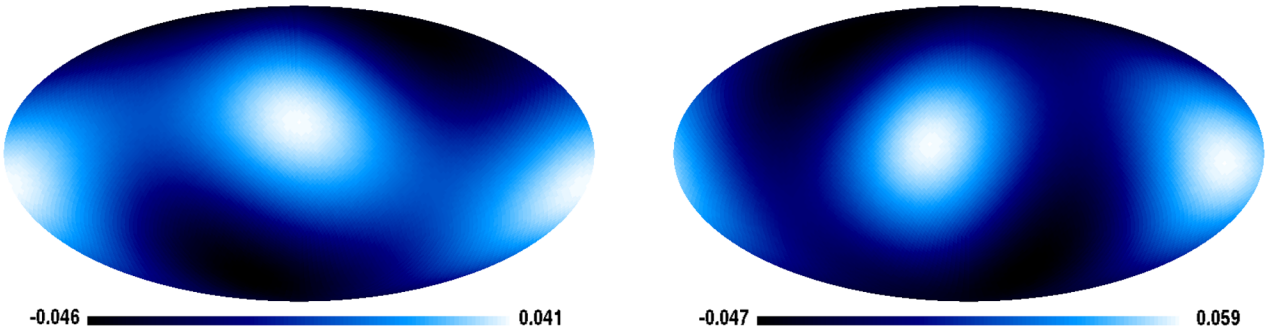

FIG. 2 (color online). The amplitude of the special quadrupole g_* estimated from the V (left) and W (right) bands of deconvolved WMAP9 maps as a function of the direction in the sky. The plot is in galactic coordinates with $l = 180°$ on the left.

TABLE I. WMAP9 V band 95% C.L. constraints on the amplitude of the special quadrupole g_* for particular preferred directions in the sky.

Preferred direction	Constraint on the amplitude g_*
$(l, b) = (96.4, 29.8)$	$-0.039 < g_* < 0.043$
$(l, b) = (96.4, 60.2)$	$-0.076 < g_* < 0.008$
$(l, b) = (186.4, 0.0)$	$-0.022 < g_* < 0.078$

presented in Table II. As a particular application of new constraints, we set limits on the constant c, a free parameter in case I of anisotropic inflation. In light of the comparison with the Planck constraints [see Eq. (53)], we also establish 68% C.L. limits,

$$-0.046 < g_* < 0.048, \tag{50}$$

obtained from the V band of the WMAP9 data.

The amplitude g_* is random in a number of realistic models and the constraints above are not applicable there. For example, this is the case of anisotropic inflation for the amplitude g_* sourced by the quantum excitations of the electric field, $\mathbf{E}_{\rm IR}$. To set limits on this class of models we slightly modify our constraining scheme. That is, we fix some value of the e-fold number $N = N_{\rm tot} - N_{\rm CMB}$ in the beginning. Using Eq. (12) with $\mathcal{P}_\zeta \approx 2.46 \times 10^{-9}$ we generate the collection of vectors $\mathbf{a}$. Each vector $\mathbf{a}$ uniquely defines the amplitude g_* and the set of coefficients $\{q_{2M}\}$. We generate anisotropic maps for each set. Finally, we compare the value of the e-fold number N estimated from the anisotropic maps with the WMAP9 estimate. We make use of the estimator (45). Limits on the relative e-fold number $N \equiv N_{\rm tot} - N_{\rm CMB}$ are given in Table II at the 95% C.L. The 68% C.L. limit is the strongest one for the V band,

$$N < 14 \cdot \left(\frac{60}{N_{\rm CMB}}\right)^2. \tag{51}$$

A similar constraint was obtained in Ref. [35] from the nonobservation of the trispectrum non-Gaussianity in the Planck data [36]; see the discussion in Sec. VI.

B. Constraints on the (pseudo)conformal universe

Now, let us turn to the models of the (pseudo)conformal universe. We start with sub-scenario A. As discussed in Sec. III C, it predicts the quadrupolar statistical anisotropy of both the general and special types. The latter appears in the nonlinear order (NLO) in the constant h, while the former is nonzero in the linear order (LO). Still, the general quadrupole makes a weaker imprint on the CMB sky than the special quadrupole. Indeed, the former is characterized by the decreasing amplitude $a(k) = H_0 k^{-1}$, which translates into the additional suppression by the CMB multipole number $l \sim k/H_0$. Consequently, we have effectively low statistics for the multipoles that are useful in the analysis and, hence, a very weak constraint on the parameter h^2. As a proof, the formal constraint $h^2 < 190$ was obtained from the V band of the WMAP7 data at the 95% C.L. Of course, we cannot trust so large an upper limit, since it violates the assumption of small statistical anisotropy made in the beginning. Rather the number "190" demonstrates the low sensitivity of the WMAP7 data towards the signal predicted.

Qualitatively, the same story repeats at the level of WMAP9 maps. To show this explicitly, we estimate the coefficients q_{LM} and C_L^q, but now with the decreasing amplitude $a(k) = H_0 k^{-1}$ in Eqs. (1) and (36). The corresponding results are shown in Fig. 3. For the value of h^2 we use the estimator (44). Next, we generate 100 sets of the coefficients q_{2M} using Eq. (24) out of some fixed value of the parameter h^2, and construct anisotropic maps for each set. We compare values of the estimator for the parameter h^2 obtained from the real data and MC-simulated anisotropic maps. The final results are presented in Table II.

Much tighter bounds are expected from the nonobservation of statistical anisotropy of the special type.

TABLE II. WMAP 95% C.L. constraints on parameters of anisotropic models from the nonobservation of statistical anisotropy in the CMB sky. These include anisotropic inflation, and sub-scenarios A and B of the (pseudo) conformal universe. Constraints in the second column are nominal in the sense that they have been obtained by a direct comparison with the anomalous quadrupole as observed in Ref. [22].

	5 yr/W	7 yr/V	9 yr/V	9 yr/W
Special quadr.	$g_* < 0.3$	⋯	$\lvert g_*\rvert < 0.072$	$\lvert g_*\rvert < 0.085$
Anis. infl. I	$c - 1 < 3.5 \times 10^{-6}$	⋯	$c - 1 < 8.3 \times 10^{-7}$	$c - 1 < 9.8 \times 10^{-7}$
Anis. infl. II	⋯	⋯	$N < 82(\frac{60}{N_{\rm CMB}})^2$	$N < 128(\frac{60}{N_{\rm CMB}})^2$
Sub-sc. A (LO)	⋯	$h^2 < 190$	$h^2 < 11$	$h^2 < 16$
Gal. gen. (LO)	⋯	$\frac{\Lambda_G^3}{f^3} < 290$	$\frac{\Lambda_G^3}{f^3} < 17$	$\frac{\Lambda_G^3}{f^3} < 24$
Sub-sc. A (NLO)	⋯	$h^2 \ln\frac{H_0}{\Lambda} < 7$	$h^2 \ln\frac{H_0}{\Lambda} < 1.2$	$h^2 \ln\frac{H_0}{\Lambda} < 2.0$
Gal. gen. (NLO)	⋯	$\frac{\Lambda_G^3}{f^3} \ln\frac{H_0}{\Lambda} < 11$	$\frac{\Lambda_G^3}{f^3} \ln\frac{H_0}{\Lambda} < 1.8$	$\frac{\Lambda_G^3}{f^3} \ln\frac{H_0}{\Lambda} < 3.0$
Sub-sc. B	⋯	$h^2 < 0.045$	$h^2 < 0.006$	$h^2 < 0.013$

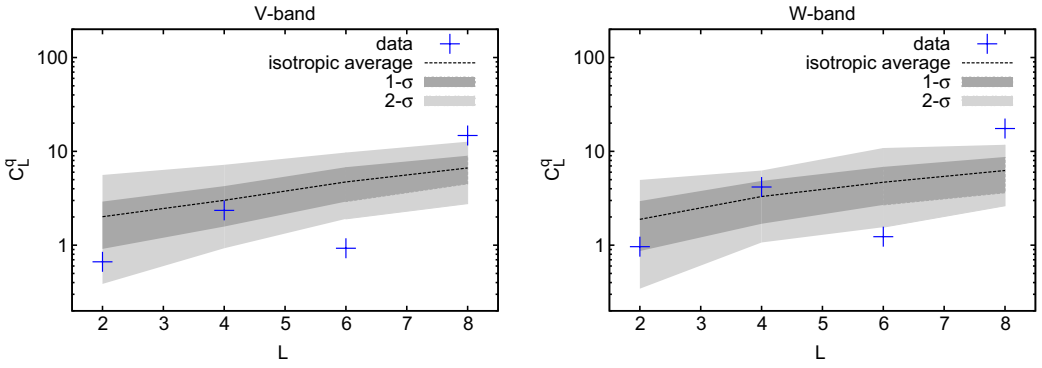

FIG. 3 (color online). The coefficients C_L^q reconstructed from the V and W bands of deconvolved WMAP9 maps in the case of $a(k) = H_0 k^{-1}$ in Eq. (1). The 1σ (dark grey) and 2σ (light grey) confidence levels are overlaid by making use of MC-generated statistically isotropic maps. The analysis is done with the WMAP9 temperature analysis mask and $l_{\max} = 400$.

Remarkably, one can derive them immediately from the upper limits on the relative e-fold number N established in the previous subsection. This is due to the correspondence between the predictions of two different setups, i.e., sub-scenario A of the (pseudo)conformal universe and case II of anisotropic inflation. The duality holds modulo the presence of the general quadrupole, which anyway produces a negligible effect for $h^2 \lesssim 1$. By exploiting Eq. (27), we obtain 95% C.L. limits on the parameter of interest, i.e., $h^2 \ln\frac{H_0}{\Lambda}$; see Table II. From Eq. (51), we also derive the 68% C.L. limit,

$$h^2 \ln\frac{H_0}{\Lambda} < 0.2.$$

Finally, using the duality (16) between the conformal rolling scenario and Galilean genesis, we convert the derived constraints into the bounds on the parameter space of the latter model; see Table II.

We conclude with constraining sub-scenario B of the (pseudo)conformal universe. We recall that statistically anisotropic effects in this case are nonzero already in the first order in the constant h. Given also the constant amplitude $a(k) = 1$, we anticipate rather strong constraints from the nonobservation of the signal predicted. We use Eq. (43) to estimate the parameter h^2. The results plotted in Fig. 4 are in excellent agreement with expectations from the isotropic hypothesis. Particular values of the parameter h^2 estimated at $L = 14$ read $h^2 = -0.0006$ (V band) and $h^2 = 0.0007$ (W band). To construct anisotropic maps, we generate a large number of sets of the coefficients q_{LM} out of some fixed value of the parameter h^2. We make use of Eq. (28). The constraints given in Table II demonstrate a roughly one-order-of-magnitude improvement as compared to our WMAP7 result.

VI. DISCUSSION

Let us discuss our constraints in light of the Planck data. The latter have the obvious advantage due to the larger number of multipoles useful in the analysis, namely $l_{\max}^{\rm Pl} \sim 2000$ as compared to $l_{\max}^{W} \sim 400$ for the WMAP9 data. Qualitatively, this implies

$$l_{\max}^{\rm Pl}/l_{\max}^{W} \sim \frac{2000}{400} = 5, \tag{52}$$

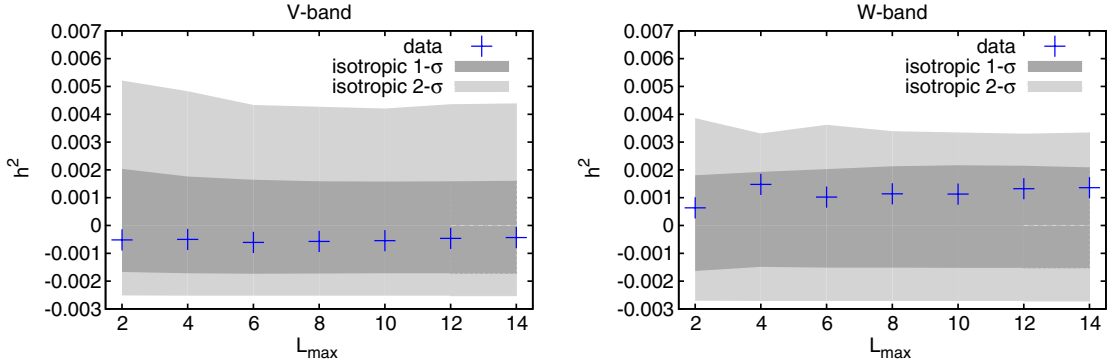

FIG. 4 (color online). Values of the estimator (43) for the parameter h^2 of the (pseudo)conformal universe, sub-scenario B, reconstructed from the V (left) and W (right) bands of deconvolved WMAP9 maps. The 1σ and 2σ confidence levels are overlaid by making use of MC-generated anisotropic maps.

i.e., a growth of the sensitivity to statistical anisotropy of the special quadrupole type. Indeed, the Fisher matrix scales as $l_{\rm max}^2$ with the maximal multipole number $l_{\rm max}$. On the other hand, the error bars for the amplitude g_* are roughly measured by $\sqrt{F_2}$. This explains the estimate (52) for the growth of sensitivity. Looking at Eq. (50), we would thus expect constraints on the amplitude g_* at the 1% level in case the signal is not observed. Recently, 68% C.L. limits appeared [37] based on the Planck 143 GHz data at the level

$$-0.014 < g_* < 0.018, \tag{53}$$

independently of the preferred direction in the sky. These Planck constraints are stronger than the limits (50) derived from the WMAP9 data by a factor of 2–3. The first Planck limits were obtained, however, using only one frequency band and a suboptimal estimator.

Based on the above, we anticipate somewhat stronger constraints with the future analysis of Planck data. Interesting consequences are expected for the duration of inflation in models with the nonminimal Maxwellian term; in particular, we expect an extremely tuned number of e-folds in those models, i.e., $N_{\rm tot} - N_{\rm CMB} \simeq \mathcal{O}(1)$. Planck data are also promising for constraining sub-scenario B of the (pseudo)conformal universe. Indeed, the sensitivity of the data to the parameter h^2 grows as $l_{\rm max}^2$. Qualitatively, this implies a bound on h^2 that is stronger by a factor of $(l_{\rm max}^{\rm Pl}/l_{\rm max}^{W})^2 \sim 25$ in the case where the signal of interest is not observed. A much weaker improvement, i.e., by a factor $l_{\rm max}^{\rm Pl}/l_{\rm max}^{W} \sim 5$, is expected for the parameter $h^2 \ln \frac{H_0}{\Lambda}$ of sub-scenario A.

We end with a few remarks. The types of statistical anisotropy studied in this paper cover most predictions that exist in the literature, but not all. For example, the model of Ref. [38] predicts a special quadrupole characterized by an increasing amplitude, i.e., $g_* \sim k^4$. This originates from the axial coupling between the inflaton and vector fields. The peculiar form of statistical anisotropy with a vanishing quadrupole term follows from inflation involving scalars with nonminimal kinetic terms [39]. In both cases, a separate data analysis is required. On the other hand, the constraints presented in Table II are easily converted into limits on the parameters of scenarios with more conventional predictions, e.g., statistical anisotropy of the ACW type. These include scenarios based on noncommutative geometry [40], p-forms [41], etc.

Although we focused on the particular prediction of statistical anisotropy, the scenarios discussed in this paper may have other interesting signatures. Indeed, anisotropic inflation gives rise to some amount of non-Gaussianities at both the bispectrum [11] and trispectrum [35] levels. These are sourced by infrared fluctuations of the electric field, and thus are highly sensitive to the duration of the inflationary phase. In Ref. [35], this simple observation was used to establish the upper limit

$$N \lesssim 17 \times \left(\frac{N_{\rm CMB}}{50}\right)^4 \cdot \left(\frac{\tau_{\rm NL}}{2800}\right). \tag{54}$$

Also, given that the Planck constraint for the trispectrum parameter $\tau_{\rm NL} < 2800$ at 95% C.L., one concludes that the constraint (54) is fairly similar to our 68% C.L. limit (51). Note, however, that the random nature of the field $\mathbf{E}_{\rm IR}$ was not accounted for in the derivation of Eq. (54). Thus, the latter is less conservative by its definition and may become weaker if the randomness is included. Other predictions of inflation with the nonminimal Maxwellian term include the anisotropy in the tensor power spectrum and the cross correlation between curvature and tensor perturbations [8,9].

Models of the (pseudo)conformal universe may also lead to potentially large non-Gaussianities [18,30,42]. In particular, the trispectrum [18,30] governed by the parameter h^2 can be used to constrain the latter from nonobservation in the Planck data. This approach appears to be especially promising in view of the fact that sub-scenario A predicts a rather weak signal of statistical anisotropy.

ACKNOWLEDGMENTS

It is a pleasure to thank Valery Rubakov, Diego Chialva, Alessandro Gruppuso, Maxim Libanov, and Federico Urban for many useful comments and stimulating discussions. We are grateful to D. Hanson for kindly providing the code for inverse variance filtering. S. R. is supported by the Belgian Science Policy (IAP VII/37). S. R. is indebted to Lund University for warm hospitality. The work of G. R. is supported in part by the RFBR grants 12-02-00653, 12-02-31776, 13-02-01293, by the Dynasty Foundation, by the grants of the President of the Russian Federation NS-5590.2012.2, MK-1170.2013.2, and by the Russian Federation Governement Grant No. 11.G34.31.0047. We acknowledge the use of the Legacy Archive for Microwave Background Data Analysis (LAMBDA), part of the High Energy Astrophysics Science Archive Center (HEASARC). HEASARC is a service of the Astrophysics Science Division at the NASA Goddard Space Flight Center. The numerical part of the work was done at the cluster of the Theoretical Division of INR RAS.

[1] R. M. Wald, Phys. Rev. D **28**, 2118 (1983).
[2] L. Ackerman, S. M. Carroll, and M. B. Wise, Phys. Rev. D **75**, 083502 (2007); **80**, 069901(E) (2009).
[3] A. Golovnev, V. Mukhanov, and V. Vanchurin, J. Cosmol. Astropart. Phys. 06 (**2008**) 009.
[4] S. Yokoyama and J. Soda, J. Cosmol. Astropart. Phys. 08 (**2008**) 005.
[5] K. Dimopoulos, M. Karciauskas, D. H. Lyth, and Y. Rodriguez, J. Cosmol. Astropart. Phys. 05 (**2009**) 013; K. Dimopoulos, M. Karciauskas, and J. M. Wagstaff, Phys. Lett. B **683**, 298 (2010); K. Dimopoulos, Int. J. Mod. Phys. D **21**, 1250023 (2012); **21**, 1292003(E) (2012).
[6] B. Himmetoglu, C. R. Contaldi, and M. Peloso, Phys. Rev. D **79**, 063517 (2009); **80**, 123530 (2009).
[7] M.-a. Watanabe, S. Kanno, and J. Soda, Phys. Rev. Lett. **102**, 191302 (2009); M.-a. Watanabe, S. Kanno, and J. Soda, Prog. Theor. Phys. **123**, 1041 (2010).
[8] A. E. Gumrukcuoglu, B. Himmetoglu, and M. Peloso, Phys. Rev. D **81**, 063528 (2010); T. R. Dulaney and M. I. Gresham, Phys. Rev. D **81**, 103532 (2010).
[9] J. Soda, Classical Quantum Gravity **29**, 083001 (2012).
[10] A. Maleknejad, M. M. Sheikh-Jabbari, and J. Soda, Phys. Rep. **528**, 161 (2013).
[11] N. Bartolo, S. Matarrese, M. Peloso, and A. Ricciardone, Phys. Rev. D **87**, 023504 (2013).
[12] D. H. Lyth and M. Karciauskas, J. Cosmol. Astropart. Phys. 05 (**2013**) 011.
[13] V. A. Rubakov, J. Cosmol. Astropart. Phys. 09 (**2009**) 030.
[14] P. Creminelli, A. Nicolis, and E. Trincherini, J. Cosmol. Astropart. Phys. 11 (**2010**) 021.
[15] K. Hinterbichler and J. Khoury, J. Cosmol. Astropart. Phys. 04 (**2012**) 023.
[16] M. Libanov and V. Rubakov, J. Cosmol. Astropart. Phys. 11 (**2010**) 045.
[17] M. Libanov, S. Ramazanov, and V. Rubakov, J. Cosmol. Astropart. Phys. 06 (**2011**) 010.
[18] P. Creminelli, A. Joyce, J. Khoury, and M. Simonovic, J. Cosmol. Astropart. Phys. 04 (**2013**) 020.
[19] S. R. Ramazanov and G. I. Rubtsov, J. Cosmol. Astropart. Phys. 05 (**2012**) 033.
[20] D. Hanson and A. Lewis, Phys. Rev. D **80**, 063004 (2009).
[21] N. E. Groeneboom and H. K. Eriksen, Astrophys. J. **690**, 1807 (2009).
[22] N. E. Groeneboom, L. Ackerman, I. K. Wehus, and H. K. Eriksen, Astrophys. J. **722**, 452 (2010).
[23] A. R. Pullen and C. M. Hirata, J. Cosmol. Astropart. Phys. 05 (**2010**) 027.
[24] D. Hanson, A. Lewis, and A. Challinor, Phys. Rev. D **81**, 103003 (2010).
[25] C. L. Bennett *et al.* (WMAP Collaboration), Astrophys. J. Suppl. Ser. **208**, 20 (2013).
[26] A. Maleknejad and M. M. Sheikh-Jabbari, Phys. Rev. D **85**, 123508 (2012).
[27] M. Osipov and V. Rubakov, JETP Lett. **93**, 52 (2011).
[28] P. A. R. Ade *et al.* (Planck Collaboration), arXiv:1303.5076.
[29] J.-L. Lehners, Phys. Rep. **465**, 223 (2008).
[30] M. Libanov, S. Mironov, and V. Rubakov, Phys. Rev. D **84**, 083502 (2011); Prog. Theor. Phys. Suppl. **190**, 120 (2011).
[31] K. M. Smith, O. Zahn, and O. Dore, Phys. Rev. D **76**, 043510 (2007).
[32] http://www.netlib.org/slatec/.
[33] http://www.gnu.org/software/gsl/.
[34] A. Lewis, A. Challinor, and A. Lasenby, Astrophys. J. **538**, 473 (2000).
[35] T. Fujita and S. Yokoyama, J. Cosmol. Astropart. Phys. 09 (**2013**) 009.
[36] P. A. R. Ade *et al.* (Planck Collaboration), arXiv:1303.5084.
[37] J. Kim and E. Komatsu, Phys. Rev. D **88**, 101301 (2013).
[38] F. R. Urban, Phys. Rev. D **88**, 063525 (2013).
[39] C. Armendariz-Picon, J. Cosmol. Astropart. Phys. 09 (**2007**) 014.
[40] E. Di Grezia, G. Esposito, A. Funel, G. Mangano, and G. Miele, Phys. Rev. D **68**, 105012 (2003); E. Akofor, A. P. Balachandran, S. G. Jo, A. Joseph, and B. A. Qureshi, J. High Energy Phys. 05 (**2008**) 092.
[41] C. Germani and A. Kehagias, J. Cosmol. Astropart. Phys. 03 (**2009**) 028; T. S. Koivisto and N. J. Nunes, Phys. Lett. B **685**, 105 (2010); Phys. Rev. D **80**, 103509 (2009); C. Germani and A. Kehagias, J. Cosmol. Astropart. Phys. 11 (**2009**) 005; T. S. Koivisto, D. F. Mota, and C. Pitrou, J. High Energy Phys. 09 (**2009**) 092; F. R. Urban, Phys. Rev. D **88**, 063525 (2013).
[42] K. Hinterbichler, A. Joyce, and J. Khoury, J. Cosmol. Astropart. Phys. 06 (**2012**) 043.